

Article

Power System Rotor Angle Stability Enhancement Using Lyapunov-Based Trajectory Tracking Controller and Model Reference Adaptive Control

Tswa-wen Pierre-Patrick Banga-Banga *, Yohan Darcy Mfoumboulou * and Carl Kriger *

Centre for Substation Automation and Energy Management Systems (CSAEMS), Department of Electrical, Electronics and Computer Engineering, Cape Peninsula University of Technology, Cape Town 7500, South Africa
* Correspondence: 211132500@mycput.ac.za (T.-w.P.-P.B.-B.); mfoumboulou@cpuc.ac.za (Y.D.M.); kriger@cput.ac.za (C.K.)

Abstract: It is vital that the synchronous generator rotor angle be kept stable to avoid disastrous consequences such as the loss of synchronism amongst generators within a power system network. Once it is unstable, the time that is taken to remedy this is advised to be 5–10 s for smaller power systems and 15–20 s for larger ones. The instability that is caused by poorly damped Low-Frequency Electromechanical Oscillations (LFEOs) may result in inter-area oscillations, where a group of generators in one area oscillates against those in another area, thus affecting the stability of the entire network. This paper explores two control architectures, namely, a nonlinear Lyapunov-based trajectory tracking controller and a Model Reference Adaptive Controller (MRAC) as options to enhance the stability of the rotor angle. The performance of each of these controllers was assessed under steady-state conditions, and then, the synchronous generator was subjected to Gaussian noise and an impulse. While the first one is aimed at emulating small variations in the system loads that are responsible for inter-area oscillations, the latter one is an attempt to explore their performance for transient stability.

Keywords: Lyapunov theory; MRAC; oscillations damping; inter-area oscillations; gaussian noise; SMIB; MATLAB/SIMULINK; trajectory tracking controller; rotor angle stability enhancement



Citation: Banga-Banga, T.-w.P.-P.; Mfoumboulou, Y.D.; Kriger, C. Power System Rotor Angle Stability Enhancement Using Lyapunov-Based Trajectory Tracking Controller and Model Reference Adaptive Control. *Energies* **2022**, *15*, 8479. <https://doi.org/10.3390/en15228479>

Academic Editor: Yacine Amara

Received: 23 September 2022

Accepted: 9 November 2022

Published: 13 November 2022

Publisher's Note: MDPI stays neutral with regard to jurisdictional claims in published maps and institutional affiliations.



Copyright: © 2022 by the authors. Licensee MDPI, Basel, Switzerland. This article is an open access article distributed under the terms and conditions of the Creative Commons Attribution (CC BY) license (<https://creativecommons.org/licenses/by/4.0/>).

1. Introduction

For every dynamical system with feedback control, stability is a crucial factor. For those systems that are categorized as Linear Time Invariant (LTI), techniques such as eigenvalue analysis, root locus, phase margins, etc., are appropriate [1]. Through the publication of “The General Problem of Motion”, Alexander Mikhailovich Lyapunov presented the general and integral methodologies for the stability of nonlinear systems as well as the quantitative and qualitative stabilization procedures that are known as linearization and direct stabilization [2,3]. Most real-world systems are intrinsically nonlinear and exhibit a variety of complex behaviors that are not seen in linear systems. In some subspaces of their nonlinear solutions, these complex behaviors are considered to be idealizations of nonlinear systems [1]. Their complex nature is illustrated by traits such as numerous equilibrium points, limit cycles, finite escape times, or chaos [1]. Lyapunov’s stability theory is crucial for the creation of nonlinear adaptive controllers [1,4–7]. As power systems are inherently nonlinear, controllers that are based on this stability theory are the best candidates to ensure their stability. Moreover, they naturally experience low-frequency electromechanical oscillations (LFEOs), which are triggered by slight changes in the system load. Undoubtedly, a change in the operating conditions leads to the emergence of contingencies such as ringdown oscillations when a state changes from stable to unstable. If it is not suitably suppressed, a quick system failure is consequently anticipated [8]. As they are the primary cause of inter-area oscillations and because they limit the generation’s

output, these oscillations represent a real threat to power system networks [9]. Moreover, they are caused by the instability of the synchronous generator rotor angle. Therefore, mitigating their effects by ensuring the stability of the rotor angle is maintained is being crucial as it may lead to a system collapse if it is not properly damped.

Various methods have been proposed to ensure the stability of the power system through decentralized architectures. To improve the grid stability, the authors of [10] suggest coordinating the dispersed controllers using constrained optimization. According to the findings, the power system's closed-loop resilience may be achieved by improving the modal performance index, which influences the controller's operation by accurately identifying the optimization constraints. Decentralized Power System Stabilizers (PSS) that employ local and remote signals to improve the damping of the inter-area oscillations are reported in [11], with each local controller having been tailored to the oscillation mode of interest. While the generator speed or the angle that is proposed act as local signals, the remote signal is selected to carry most of the data for the particular inter-area mode. Numerous studies, including [12], have demonstrated the viability of the electrical power that is transferred at the tie line. A new method for reducing Low-Frequency Electromechanical Oscillations (LFEOs) was introduced in [13], and it combines PSS with a rotor angle controller whose input comes from a Phasor Measurement Unit (PMU). Instead of using the generator speed as an input, the governor uses the measured absolute rotor angle. By removing the integration block from the previously suggested structure, [14] offered a modified rotor angle controller as an extension of the work that was conducted by the authors of [12], and they took into account the influence of the penetration of Distributed Generation (DG) on the frequency fluctuation. The integration block is said to cause negative damping torque at low frequency inputs and frequent turbine valve adjustments. It is claimed that this suggested structure, which is also known as Rotor Angle Droop (RAD) control, would more effectively reduce the LFEOs while still maintaining the generation load balance and the system frequency at the rated value. The use of an Adaptive Model Predictive Controller (AMPC) is reported in [15] where it is proposed for the design of a measurement-based indirect adaptive wide-area supplemental damping controller. There, a Recursive Polynomial Model Estimator (RPME) was used to accomplish the online identification of plant model parameters. Other strategies such as coordinating the governors of the generators and PSSs to mitigate the inter-area oscillations are described in [15]. The role of the governor in the damping of these oscillations is highlighted in [13] and [14], but in contrast to their method, which uses the (rotor) angle as the input, the typical structure—that is, the rotor speed deviation—is used.

However, in most of the aforementioned decentralized schemes, the authors either considered optimization, or opted to enhance the performance of the PSSs by utilizing them in conjunction with some linear control strategies. As the dynamic equations of the synchronous generator are nonlinear, this paper explores instead two widely used nonlinear control strategies: the Lyapunov-based trajectory tracking controller and MRAC to improve the stability of the rotor angle.

Trajectory tracking controllers based on Lyapunov have been extensively used to ensure a given system's output following that of the chosen reference model. With applications in robotics [16,17], the nonlinear control of Magnetic Levitation [18], or wastewater control [19], these controllers have ensured that asymptotic stability was achieved. The use of adaptive control in power system has been reported as early as in the 1980s in [20] which presented a comparative study between adaptive-based stabilizers with the one that was based on fixed gains and their effects on the generator excitation control. The authors opted against the use of an algorithm with implicit identification such as the MRAC, but instead they proposed explicitly identified controllers such as the Optimal Linear Quadratic (LQ) and Pole Assigned (PA) Controllers. In their paper, the adaptive controller is configured as a transient gain stabilizer. The authors of [21] presented a decentralized multivariable self-tuning adaptive controller to improve the dynamic stability of power systems. Unlike many before them, such as in [20] where the controllers were applied on the excitation based

on a Single-Input/Single-Output (SISO) configuration, a Single-Input/Multiple-Output (SIMO) was considered, instead with the excitation signal, to be the input and the terminal voltage, shaft speed, and output power were considered to be the outputs. In a similar way to [20,21], we advocated against MRAC due to the difficulty in the choice of an appropriate reference model. However, as highlighted in [22], the 3rd and 4th order representations of synchronous generators are sufficient for the controller design. The valid concern that has been raised by the aforementioned authors is thus, reduced to finding a suitable 3rd order or 4th order reference model. The application of MRAC in power system stability can be found in [23] where it is used for the design of an adaptive scheme of a Permanent Magnet (PM) synchronous motor, [24] to enhance the Low-Voltage Ride Through (LVRT) capability for the grid integration of wind energy systems, [25] for the transient stability enhancement of Virtual Synchronous Generators (VSG), and [26] for outer Photovoltaic (PV) voltage control loop and inner grid control.

In a similar way to [21], a decentralized adaptive control algorithm is presented in this manuscript to enhance the stability of the rotor angle. However, as opposed to the SIMO configuration that is reported therein, a Multiple-Input/Multiple-Output (MIMO) configuration is instead proposed with no PSS. Moreover, as the 3rd and 4th order model representations of the synchronous generator are suitable for the controller design [22] and by extending the work in [24–27], a MRAC scheme is proposed to address the small-signal rotor angle stability problem. Furthermore, a Lyapunov-based nonlinear trajectory-tracking algorithm is explored and its performance to ensure the stability of the rotor angle is compared to that of the MRAC.

2. Motivation

Rotor stability must be monitored and managed in real-time due to the possible harm that might result from its instability. As underlined by the authors of [22], oscillations involving a set of generators in one location, oscillating against another group in another area, are responsible for system breakdowns.

3. Contribution of the Manuscript

This paper extends the work in [24–27] by comparing the performance of a Lyapunov-based trajectory tracking controller with that of a MRAC algorithm in ensuring the stability of the synchronous generator rotor angle. In lieu of a SISO or a SIMO as in [20,21], a MIMO is proposed with the field voltage and mechanical power to be the inputs, with the electrical power and rotor angle as the outputs. Similar to that in [21], a decentralized MRAC algorithm is proposed. With decentralized control architectures, some people have considered modified PSSs with dual inputs [28], while others have explored other nonlinear methods including Lyapunov-based PSS [29]. In contrast to the latter, the explored Lyapunov-based controller in this paper has been applied to the synchronous generator modeled in its 3rd order without any PSS.

The novelty of this paper is as below:

- The exploration of a nonlinear trajectory-tracking algorithm for power systems small-signal rotor angle stability enhancement.
- The application of a MRAC for power systems small-signal rotor angle stability enhancement.
- A comparison of the performance between a nonlinear trajectory-tracking and a MRAC algorithm for power systems small-signal rotor angle stability enhancement.
- The introduction of Gaussian noise as a disturbance to mimic the disturbances that are caused by small variations in the system load.

4. Delimitations and Constraints

4.1. Delimitations

While we explore both of the control algorithms, no PSS is considered.

4.2. Constraints

The results presented can be replicated using the synchronous generator parameters in the Appendix A. As opposed to MRAC where the performance is guaranteed for any value of the adaptation rate $\in [2, 100]$, a gain of 4.5 is required for the trajectory-tracking Lyapunov-based controller. In the absence of any reference in the literature regarding the computation of the suitable gain for Lyapunov-based controllers, empirical methods will be required for generators with different parameters than the ones that are used in this paper.

5. Organization of the Manuscript

The remainder of the paper is structured as follows: Section 6 presents an overview of the nonlinear systems, and Section 7 introduces the Lyapunov stability theory. The dynamics of the synchronous generator are presented in Section 8, while Sections 9 and 10 cover the aspects of the design of the nonlinear trajectory-tracking algorithm and MRAC, respectively. Section 11 shows the results of the simulation when both of the algorithms were applied to the synchronous generator rotor angle. The discussions are presented in Section 12, with the conclusions being in Section 13. Section 14 presents the recommendations and future work.

6. Overview of Nonlinear Systems

Nonlinear systems differ significantly from linear systems due to their plethora of complex behaviors [1,30]. In contrast to LTI systems, a given nonlinear system can have several equilibrium points, and its phase plane analysis is comparable to that of its linearized version since its local behaviors can be approximated by the linearized one in the region of the equilibrium points. Furthermore, unlike linear systems, where instability indicates that the solution expands exponentially as $t \rightarrow \infty$ owing to unstable poles in the right half plane, resulting in unbounded signals, the instability in the nonlinear systems does not necessarily result in unbounded signals [1,2]. Aside from the several separate equilibrium points, two more notable characteristics of such systems are noted by [1]:

Finite escape time: A nonlinear system's ability to become unbounded in a finite time span. This phenomenon occurs exclusively in unstable linear systems as the time approaches infinity.

Limit cycle: This is described as "a periodic nonlinear solution represented by a closed trajectory in the phase plane so that all trajectories in its proximity either converge to it or diverge from it", and it can either be stable, unstable, or neutral depending on the trajectories of the solution in its vicinity.

7. Lyapunov Stability Theory

The stability of a dynamic system may be evaluated by changing a single scalar (energy) function, which is based on a physical phenomenon that links a certain mechanical (spring-mass-damper) system equilibrium to the decrease in its "measure of energy" [2,31]. The Lyapunov function may be any positive-defined function that fulfils the (semi)-definiteness of its time derivative, which is unlike physical systems where this energy function is exclusive [1]. It is comparable to the mechanical system's energy concept, where the following observations may be made:

- The positivity of the energy function.
- The negative semi-definiteness of the time rate of the energy function and the stability of the equilibrium are linked.

Using a family of positive-definite functions, Lyapunov realized that it was possible to prove the stability of a particular system without having a complete understanding of the system's energy [1]. Various theorems are derived from this theory such as the Lyapunov theorem for local stability, the Lyapunov theorem for exponential stability, the Barbashin–Krasovkii theorem for global asymptotic stability, the Lasalle's invariant set theorem, and the Barbalat's lemma. Details around each of these can be found in [1,2,26,28]. Nevertheless, and as emphasized in [1], "The Lyapunov stability theory is the foundation of nonlinear systems and adaptive control theory". Moreover, the following can be said:

- i. Global stability analysis is facilitated by the Barbashin–Krasovskii theorem.
- ii. LaSalle’s invariant set theorem is a useful technique for analysing systems which have invariant sets.
- iii. Uniform stability, uniform bounding, and uniform ultimate boundness are concepts that are used to evaluate the stability of non-autonomous systems.
- iv. Barbalat’s theorem allows for a more in-depth analysis of the stability of adaptive control systems in relation to the uniform continuity of a real-valued function.

8. Synchronous Generator Dynamics

Other than the 2nd order representation of the synchronous generator dynamics which is also referred to as the Swing Equation, the higher orders such as the 3rd, 4th, 5th, and 7th ones could also be used to describe it. Details regarding them as well as the fields of study that each of them is best suited for can be found in [22,32,33]. The study of the generator control systems and their synthesis as well as the dynamic analysis of the small-signal stability are both stated to be appropriate applications for the third order model [22]. As for the 4th order model, it is sufficiently accurate to analyse electromechanical dynamics [32,34], and as emphasized by [22], it is appropriate for modelling the generator over the whole spectrum of (local and inter-area) electromechanical oscillations. Both the 3rd and 4th order model representations of the synchronous generator’s dynamics are used throughout this paper for the purpose of the controller design.

8.1. Synchronous Generator 3rd Order Representation

The equations that describe this model are as follows:

$$\dot{\delta} = \omega \quad (1)$$

$$\dot{\omega} = \frac{1}{J}(T_m - P_e - D\omega) \quad (2)$$

$$\dot{e}'_q = \frac{1}{T'_{do}} \left(E_{FD} - e'_q - (x_d - x'_d) i_d \right) \quad (3)$$

where

$$i_d = \frac{e'_q - V \cos \delta}{x'_q}$$

$$i_q = \frac{V \sin \delta}{x_q}$$

$$P_e \cong \frac{V}{x'_d} e'_q \sin \delta + \frac{V^2}{2} \left(\frac{1}{x'_q} - \frac{1}{x'_d} \right) \sin(2\delta)$$

δ : rotor angle.

ω : rotor speed.

i_d : d-axis current.

i_q : q-axis current.

V : Transformer’s terminal voltage.

E_{FD} : induced emf by the field current (field voltage).

T'_{do} : d-axis open-circuit time constant.

e'_q : q-axis transient emf.

D : damping coefficient.

P_e : air-gap power of the generator.

$$\text{Let } \underline{x} = \begin{bmatrix} x_1 \\ x_2 \\ x_3 \end{bmatrix} = \begin{bmatrix} \delta \\ \omega \\ e'_q \end{bmatrix}, \text{ and } \underline{u} = \begin{bmatrix} u_1 \\ u_2 \end{bmatrix} = \begin{bmatrix} E_{FD} \\ P_m \end{bmatrix}.$$

Because magnetic saturation is ignored in this model, x_d , x_q , and x'_d can be assumed to be constant. However, the x_d , x_q , and x'_d that are used in Equations (1)–(3) are the augmented reactances with the line and transformer reactances added onto them [35,36]. The state-space model is as in Equation (4):

$$\dot{\underline{x}} = \begin{bmatrix} 0 & 1 & 0 \\ 0 & -\frac{D}{J} & 0 \\ 0 & 0 & \frac{1}{T'_{do}} \left(\frac{x_d}{x'_d} \right) \end{bmatrix} \begin{bmatrix} \delta \\ \omega \\ e'_q \end{bmatrix} + \begin{bmatrix} 0 & 0 \\ 0 & \frac{1}{J} \\ \frac{1}{T'_{do}} & 0 \end{bmatrix} \begin{bmatrix} E_{FD} \\ P_m \end{bmatrix} + \begin{bmatrix} 0 \\ -\frac{1}{J} \left(\frac{V}{x'_d} e'_q \sin(\delta) + \frac{V^2}{2} \left(\frac{1}{x_q} - \frac{1}{x'_d} \right) \sin(2\delta) \right) \\ \frac{1}{T'_{do}} \left(\frac{x_d - x'_d}{x'_d} \right) V \cos(\delta) \end{bmatrix} \quad (4)$$

This can be written in the form of $\dot{\underline{x}} = A\underline{x} + B\underline{u} + \underline{f}(\delta)$, where $\underline{f}(\delta)$ is a vector with nonlinear elements. Given that the electrical power and the generator rotor angle are used as elements of the output vector, its expression may be written as:

$$\underline{y} = \begin{bmatrix} \delta \\ P_e \end{bmatrix} = \begin{bmatrix} 1 & 0 & 0 \\ \frac{V^2}{2\delta} \left(\frac{1}{x'_q} - \frac{1}{x'_d} \right) \sin(2\delta) & 0 & \frac{V}{x'_d} \sin(\delta) \end{bmatrix} \begin{bmatrix} \delta \\ \omega \\ e'_q \end{bmatrix} \quad (5)$$

with $\underline{y} \in R^2$ being the generator output.

8.2. Synchronous Generator 4th Order Representation

As illustrated in [32,37,38], the synchronous generator's 4th order model may be thought of as an extension of the 3rd order model, with the damper winding in the q-axis being taken into account. This may be expressed as [32]:

$$\underline{x} = [\delta \ \omega \ e'_d e'_q]^T = [x_1, x_2, x_3, x_4] \quad (6)$$

$$\dot{x}_1 = \omega_0 x_2 \quad (7)$$

$$\dot{x}_2 = \frac{1}{J} (T_m - T_e - D x_2) \quad (8)$$

$$\dot{x}_3 = \frac{1}{T'_{qo}} (-x_4 + (x_q - x'_q) i_q) \quad (9)$$

$$\dot{x}_4 = \frac{1}{T'_{do}} (E_{fd} - x_3 - (x_d - x'_d) i_d) \quad (10)$$

where

$$i_d = \frac{e'_q - V \cos \delta}{x'_q}$$

$$i_q = \frac{V \sin \delta - e'_d}{x'_q}$$

$$P_e \cong \frac{V}{x'_d} e'_q \sin \delta - \frac{V}{x'_q} e'_d \cos \delta + \frac{V^2}{2} \left(\frac{1}{x'_q} - \frac{1}{x'_d} \right) \sin(2\delta)$$

δ : rotor angle

ω : rotor speed

i_d : d-axis current

i_q : q-axis current

V : Transformer's terminal voltage

E_{FD} : induced emf by the field current (field voltage)

T'_{do} : d-axis open-circuit time constant

e'_q : q-axis transient emf

e'_d : d-axis transient emf

D : damping coefficient

P_e = air-gap power of the generator.

Let $\underline{x} = \begin{bmatrix} x_1 \\ x_2 \\ x_3 \\ x_4 \end{bmatrix} = \begin{bmatrix} \delta \\ \omega \\ e'_d \\ e'_q \end{bmatrix}$ and $\underline{u} = \begin{bmatrix} u_1 \\ u_2 \end{bmatrix} = \begin{bmatrix} E_{FD} \\ P_m \end{bmatrix}$, and the state-space representation can be written as in Equation (11):

$$\dot{\underline{x}} = \begin{bmatrix} 0 & 1 & 0 & 0 \\ 0 & \frac{-D}{J} & 0 & 0 \\ 0 & 0 & -\frac{1}{x'_q T_{qo}}(x'_q + x_q - x'_d) & 0 \\ 0 & 0 & 0 & -\frac{1}{T'_{do}}\left(\frac{x'_d}{x'_d}\right) \end{bmatrix} \begin{bmatrix} \delta \\ \omega \\ e'_d \\ e'_q \end{bmatrix} + \begin{bmatrix} 0 & 0 \\ 0 & -\frac{1}{J} \\ 0 & 0 \\ \frac{1}{T'_{do}} & 0 \end{bmatrix} \begin{bmatrix} E_{FD} \\ P_m \end{bmatrix} + \begin{bmatrix} 0 \\ \frac{1}{J} \left(\frac{e'_d V}{x'_q} \cos \delta - \frac{e'_q V}{x'_d} \sin \delta - \frac{V^2}{2} \sin 2\delta \left(\frac{1}{x'_q} - \frac{1}{x'_d} \right) \right) \\ \frac{V}{T_{qo}} \left(\frac{x_q - x'_d}{x'_q} \right) \sin \delta \\ \frac{V}{T'_{do}} \left(\frac{x'_d}{x'_d} - 1 \right) \cos \delta \end{bmatrix} \quad (11)$$

The above equation can be written in the form of:

$$\dot{\underline{x}} = A\underline{x} + B\underline{u} + \underline{f}(\delta) \quad (12)$$

where $\underline{f}(\delta)$ is a vector of the nonlinear elements.

Assuming that the generator rotor angle and the (active) electrical power are the outputs, it can be written as [9]:

$$\underline{y} = \begin{bmatrix} \delta \\ P_e \end{bmatrix} = \begin{bmatrix} 1 & 0 & 0 & 0 \\ \frac{V^2}{2} \left(\frac{1}{x'_q} - \frac{1}{x'_d} \right) \sin 2\delta & 0 & \frac{V \cos \delta}{x'_q} & \frac{V \sin \delta}{x'_d} \end{bmatrix} \begin{bmatrix} \delta \\ \omega \\ e'_d \\ e'_q \end{bmatrix} \quad (13)$$

9. Design of a Lyapunov-Based Trajectory Tracking Controller

As highlighted in Section 8, the 3rd and 4th orders of the synchronous generator can be used in the design of the controllers. A nonlinear servo-based reference model controller is described in this section. Following a brief overview of the generator’s dynamics, considerations concerning the development of the reference model are presented.

9.1. Reference Model-Based Closed-Loop Control System

When we utilize the objective to verify that a provided system’s output is consistent with the same target, the reference model is said to determine the performance of the very given system [39]. The aforementioned principle underpins the design of the generator’s controller. The output behavior of the generator closed-loop system must match that of the reference model. As a result, the controller must be designed in such a manner that it generates a signal that causes the system’s output to mirror that of the reference model, as shown in Figure 1.

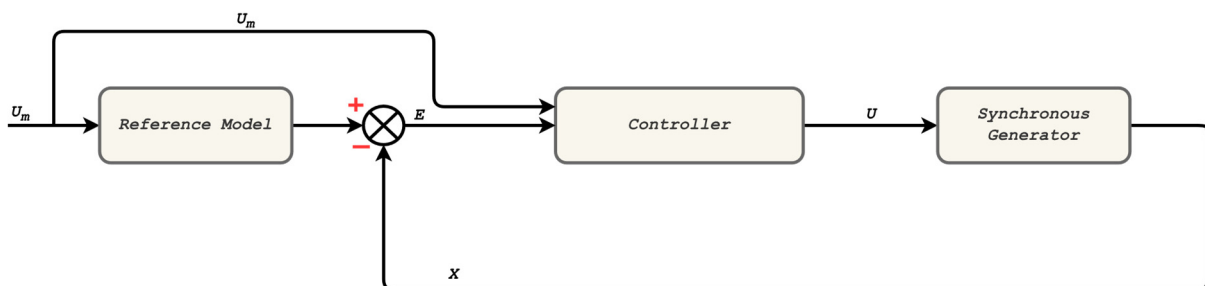


Figure 1. Proposed Lyapunov-based architecture. where $\underline{u}_m \in \mathbb{R}^m$ is the reference model’s control vector input, $\underline{u} \in \mathbb{R}^m$ the controller’s output, and $e \in \mathbb{R}^n$ the error between the desired and the generator’s state vectors.

The reference model, which is assumed to be linear in this study, is given by the following equations:

$$\dot{\underline{x}}_m = \underline{A}_m \underline{x}_m + \underline{B}_m \underline{u}_m \tag{14}$$

$$\underline{y}_m = \underline{C} \underline{x}_m \tag{15}$$

where:

$\underline{x}_m \in \mathbb{R}^n$ is the reference model’s state vector.

$\underline{u}_m \in \mathbb{R}^m$ is the reference model’s control vector.

$\underline{A}_m \in \mathbb{R}^{n \times n}$ is the reference’s model state matrix.

$\underline{B}_m \in \mathbb{R}^{n \times m}$ is the reference’s model control matrix.

While \underline{A}_m is assumed to be a *Hurwitz matrix* in order for the reference model system to have an asymptotically stable equilibrium state, the control signal \underline{u}_m is chosen in such a way that \underline{x}_m follows a desirable trajectory, and as seen in Figure 1, the generator’s state will then follow the same behavior [9]. Equations (14) and (15) determine that the reference model is a linear system. As a result, preserving its stability necessitates the use of linear control techniques. To fulfil the overall robustness that is required, the type 1 servo for the type 0 plant regulator structure is used for the calculation of the control signal \underline{u}_m .

9.2. Nonlinear Controller

This sub-section discusses the approach that can be used to develop the nonlinear linearizing controller based on a reference model and the Lyapunov stability (direct method) theory, as well as a linear controller which aims to enhancing the closed-loop system’s performance. The nonlinear controller is designed to ensure that the Single Machine Infinite Bus (SMIB) system stays stable when it is subjected to disturbances, whereas the type 1 servo for type 0 plant is employed to maintain the stability of the reference model. Figure 2 depicts the stages that are involved in the controller’s design.

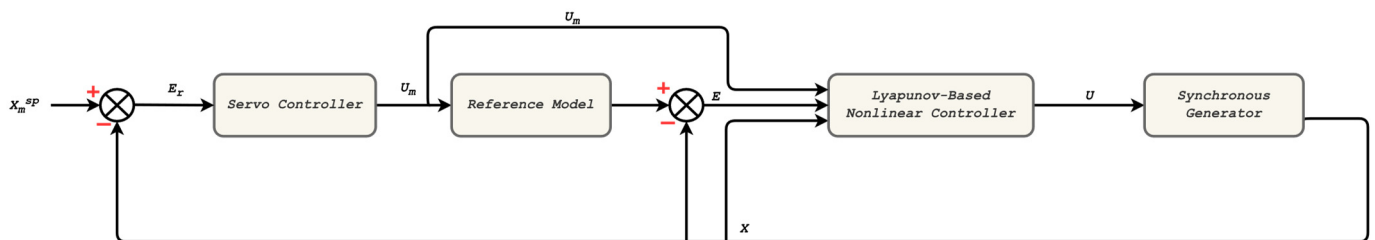


Figure 2. Overall structure of the Lyapunov-based trajectory tracking controller.

9.3. Lyapunov Functional Candidate

Let V , which is a positive definite and decrescent function, be used as the Lyapunov candidate.

$$V(t) = \underline{e}^T \underline{P} \underline{e} \tag{16}$$

where $\underline{P} \in \mathbb{R}^{n \times n}$ is a positive definite real symmetrical matrix.

9.4. Calculation of the First Derivative of the Lyapunov Function

The first derivative of the Lyapunov function that is described in Equation (16) is:

$$\dot{V}(t) = \dot{\underline{e}}^T \underline{P} \underline{e} + \underline{e}^T \underline{P} \dot{\underline{e}} \tag{17}$$

After the substitution of the expression from Equation (16), the following two expressions for the Lyapunov derivative are obtained [9]:

$$\Leftrightarrow \dot{V}(t) = \left(\underline{A}_m \underline{e} + \underline{A}_m \underline{x} + \underline{B}_m \underline{u}_m - \underline{A} \underline{x} - \underline{B} \underline{u} - \underline{f}(\delta) \right)^T \underline{P} \underline{e} + \underline{e}^T \underline{P} \left(\underline{A}_m \underline{e} + \underline{A}_m \underline{x} + \underline{B}_m \underline{u}_m - \underline{A} \underline{x} - \underline{B} \underline{u} - \underline{f}(\delta) \right) \tag{18}$$

$$\Leftrightarrow \dot{V}(t) = \underline{e}^T A_m^T P \underline{e} + \underline{x}^T A_m^T P \underline{e} + \underline{u}_m^T B_m^T P \underline{e} - \underline{x}^T A^T P \underline{e} - \underline{u}^T B^T P \underline{e} - \underline{f}(\delta)^T P \underline{e} + \underline{e}^T P A_m \underline{e} + \underline{e}^T P A_m \underline{x} + \underline{e}^T P B_m \underline{u}_m - \underline{e}^T P A \underline{x} - \underline{e}^T P B \underline{u} - \underline{e}^T P \underline{f}(\delta) \quad (19)$$

Considering $\underline{e}^T A_m^T P \underline{e} + \underline{e}^T P A_m \underline{e} = \underline{e}^T (A_m^T P + P A_m) \underline{e}$, then the following expression is obtained:

$$\dot{V}(t) = \underline{e}^T P (A_m^T P + P A_m) \underline{e} + 2\Gamma \quad (20)$$

where:

$$2\Gamma = (\underline{x}^T A_m^T P \underline{e} + \underline{u}_m^T B_m^T P \underline{e} - \underline{x}^T A^T P \underline{e} - \underline{u}^T B^T P \underline{e} - \underline{f}(\delta)^T P \underline{e}) + (\underline{e}^T P A_m \underline{x} + \underline{e}^T P B_m \underline{u}_m - \underline{e}^T P A \underline{x} - \underline{e}^T P B \underline{u} - \underline{e}^T P \underline{f}(\delta)) \quad (21)$$

In order to have $\underline{e}^T P$ at the beginning of Equation (21), the expression $(\underline{x}^T A_m^T P \underline{e} + \underline{u}_m^T B_m^T P \underline{e} - \underline{x}^T A^T P \underline{e} - \underline{u}^T B^T P \underline{e} - \underline{f}(\delta)^T P \underline{e})$ is transposed. This results in the following:

$$2\Gamma = (\underline{e}^T P A_m \underline{x} + \underline{e}^T P B_m \underline{u}_m - \underline{e}^T P A \underline{x} - \underline{e}^T P B \underline{u} - \underline{e}^T P \underline{f}(\delta)) + (\underline{x}^T A_m^T P \underline{e} + \underline{u}_m^T B_m^T P \underline{e} - \underline{x}^T A^T P \underline{e} - \underline{u}^T B^T P \underline{e} - \underline{f}(\delta)^T P \underline{e}) \quad (22)$$

$$\Rightarrow 2\Gamma = 2\underline{e}^T P (A_m \underline{x} + B_m \underline{u}_m - A \underline{x} - B \underline{u} - \underline{f}(\delta)) \quad (23)$$

Finally,

$$\Gamma = \underline{e}^T P (A_m \underline{x} + B_m \underline{u}_m - A \underline{x} - B \underline{u} - \underline{f}(\delta)) \quad (24)$$

9.5. Determination of the Nonlinear Controller Expression

Based on Barbalat's lemma, $\dot{V} < 0$ and from Equation (20) it can be written [9]:

$$\underline{e}^T P (A_m^T P + P A_m) \underline{e} + 2\Gamma < 0 \quad (25)$$

Considering that the reference model is selected to be stable, i.e., $\underline{e}^T (A_m^T P + P A_m) \underline{e} < 0$, $\Gamma < 0$ would ensure that the generator is asymptotically stable at large [9]. To make the generator's output follow the desired behavior of the reference model, the control signal \underline{u} must be computed in such a way that $\Gamma < 0$, i.e., [9]:

$$\begin{aligned} \underline{e}^T P (A_m \underline{x} + B_m \underline{u}_m - A \underline{x} - B \underline{u} - \underline{f}(\delta)) &< 0 \\ \Leftrightarrow \underline{e}^T P (A_m \underline{x} + B_m \underline{u}_m - A \underline{x} - \underline{f}(\delta)) &< \underline{e}^T P B \underline{u} \end{aligned} \quad (26)$$

To derive the expression of \underline{u} , $\underline{e}^T P B$ needs to be made into an identity matrix, and since $\underline{e}^T P B \in \mathbb{R}^{1 \times 2}$, a transformation is needed to make it quadratic for further processing [9]. This is achieved by multiplying Equation (26) with the transpose of $\underline{e}^T P B$ [9]:

$$(\underline{e}^T P B)^T \underline{e}^T P (A_m \underline{x} + B_m \underline{u}_m - A \underline{x} - \underline{f}(\delta)) = (\underline{e}^T P B)^T (\underline{e}^T P B) \underline{u} \quad (27)$$

The matrix $(\underline{e}^T P B)^T \underline{e}^T P \in \mathbb{R}^{2 \times 2}$, and multiplying it by its inverse would produce an identity matrix. This is shown through the derivations below:

$$\left[(\underline{e}^T P B)^T \underline{e}^T P \right]^{-1} (\underline{e}^T P B)^T \underline{e}^T P (A_m \underline{x} + B_m \underline{u}_m - A \underline{x} - \underline{f}(\delta)) < \left[(\underline{e}^T P B)^T \underline{e}^T P \right]^{-1} (\underline{e}^T P B)^T (\underline{e}^T P B) \underline{u} \quad (28)$$

Finally,

$$\underline{u} > \left[(\underline{e}^T PB)^T \underline{e}^T PB \right]^{-1} (\underline{e}^T PB)^T \underline{e}^T P (A_m \underline{x} + B_m \underline{u}_m - A \underline{x} - \underline{f}(\delta)) \tag{29}$$

Figure 2 which is an extension of Figure 1 illustrates the overall structure of the proposed control scheme.

10. Design of a Model Reference Based Adaptive Controller

10.1. Introduction

In this section, a Linear Quadratic Regulator (LQR)-based reference model adaptive controller is presented. Though for the 3rd order model a servo could be used as the reference model’s controller, no feedback nor feedforward gains can be obtained for the 4th order model such that:

$$A - BK_x = A_m \tag{30a}$$

$$BK_r = B_m \tag{30b}$$

where:

A_m : is the reference model system matrix.

B_m : is the reference model input matrix.

K_x : is the feedback gain matrix.

K_r : is the feedforward gain matrix.

This is due to the uncontrolled subspaces in the system matrix of the linearized 4th order model. Controlling the reference model necessitates the use of a different kind of controller. Thus, we used the LQR for its choice and control. The approach that was taken for the design of the MRAC architecture is illustrated in Figure 3.

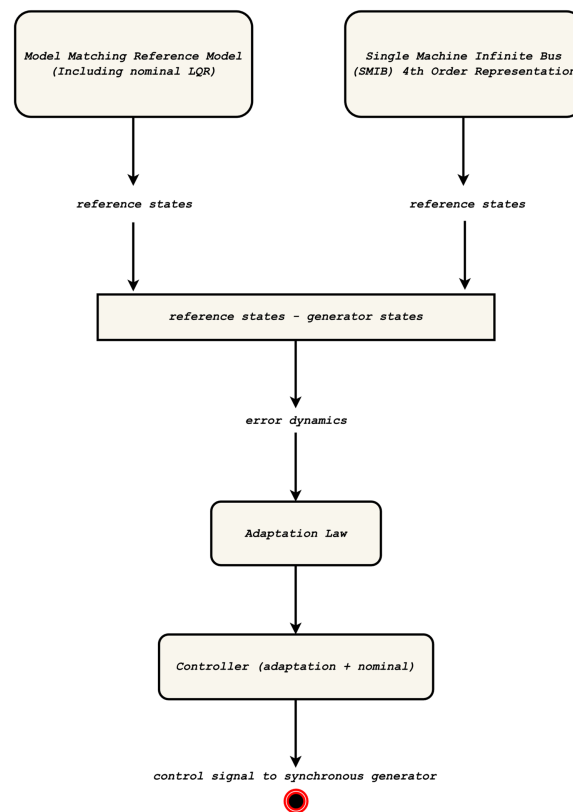


Figure 3. MRAC architecture for rotor angle stability enhancement.

10.2. Nominal Controller Structure

Given that the goal is to find matrices K_1 and K_2 such that $A - BK_1 = A_m$ and $BK_2 = B_m$, where K_1 represents the feedback gain, K_2 represents the feedforward gain, and A_m and B_m represent the reference system matrix and reference control matrices, respectively [12], the quadratic optimal control problem may be solved using the MATLAB script below, taking into account the generator settings that are listed in the Appendix A.

MATLAB Script 1

```
A = [0 1 0 0;0 0 0 0;0 0 -6.375 0;0 0 0 0.75];
B = [0 0;0 0.21;0 0;0.125 0];
C = [1 0 0 0;2.458 0 -1.326 2.28];
R = eye(2);
Q = 100 * CT * C; % moderately higher value of tau
[K,P,E] = lqr(A,B,C,Q,R);
```

The script above computes the real symmetric matrix P and optimal control feedback gain K .

$$P = \begin{bmatrix} 290.5799 & 83.6609 & -37.0418 & 159.1003 \\ 83.6606 & 59.0966 & -2.4773 & 29.1826 \\ -37.0418 & -2.4773 & 12.4794 & -32.4421 \\ 159.1003 & 29.1826 & -32.4421 & 230.1267 \end{bmatrix}$$

$$K = \begin{bmatrix} 19.8875 & 3.6478 & -4.0553 & 28.7658 \\ 17.5688 & 12.4103 & -0.5202 & 6.1283 \end{bmatrix}$$

Yet, the closed-loop response of this linear controller, as shown in Figure 4, has a significant steady-state error. The amplitude of this error is more than 0.9 units.

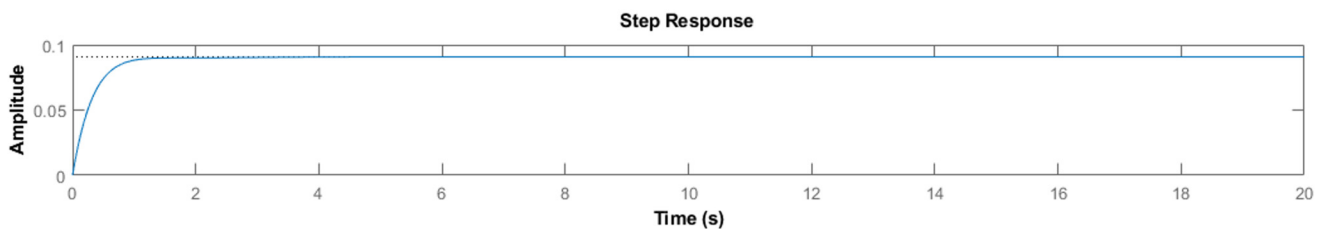


Figure 4. Output response with $E_{FD} = 1$, $P_m = 1$.

Therefore, changes to script 1 are required to address this as shown below:

MATLAB Script 2

```
A = [0 1 0 0;0 0 0 0;0 0 -6.375 0;0 0 0 0.75];
B = [0 0;0 0.21;0 0;0.125 0];
C = [1 0 0 0;2.458 0 -1.326 2.28];
R = eye(2);
Q = 100 * CT * C; % moderately higher value of tau
[K1,P,E] = lqr(A,B,C,Q,R);
% Introduce a feedforward gain that cancels the steady-state error
K2 = -inv(C * (inv(A - B*K1) * B))
```

Figure 5 shows the corrected output response.

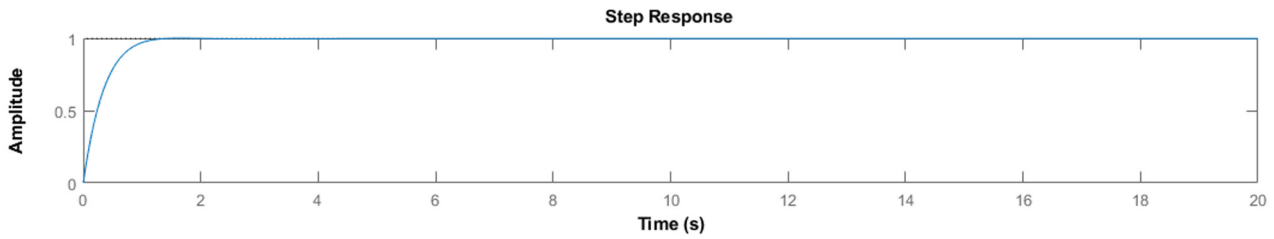


Figure 5. Corrected output response with $E_{FD} = 1, P_m = 1$.

10.3. Adaptation Law

By defining $\tilde{\theta}(t) = \theta(t) - \theta^*$ as the estimation error, the closed-loop synchronous generator model is expressed as [9]:

$$\dot{\underline{x}} = (A + BK_x)\underline{x} + BK_r r - B^T (BB^T)^{-1} \tilde{\theta}^T \Phi(x) \tag{31}$$

Thus, the closed-loop tracking error is described as in Equation (32), which is below [9]:

$$\dot{\underline{e}} = \underline{\dot{x}}_m - \dot{\underline{x}} = A_m \underline{e} + B^T (BB^T)^{-1} \tilde{\theta}^T \Phi(x) \tag{32}$$

By choosing the following Lyapunov candidate in [1]:

$$\dot{V} = -\Gamma \Phi(x) e^T P B^T (BB^T)^{-1} \tag{33}$$

and from the Barbalat’s lemma, the tracking error can be shown to be asymptotically stable with $e(t) \rightarrow 0, \forall t \rightarrow \infty$.

11. Performance of the Lyapunov-Based Trajectory Tracking Controller and MRAC for the Synchronous Generator Rotor Angle Stability Enhancement

The performance of the Lyapunov-based trajectory controller and that of the MRAC are presented in the form of case studies. These controllers are evaluated in a steady state as shown in Figure 6 as well as when they were subjected to a set of contingencies such as setpoint changes, faults, and Gaussian noise. These disturbances were either applied individually as seen in Case Study 2 or in conjunction with the others as in Case Study 3.

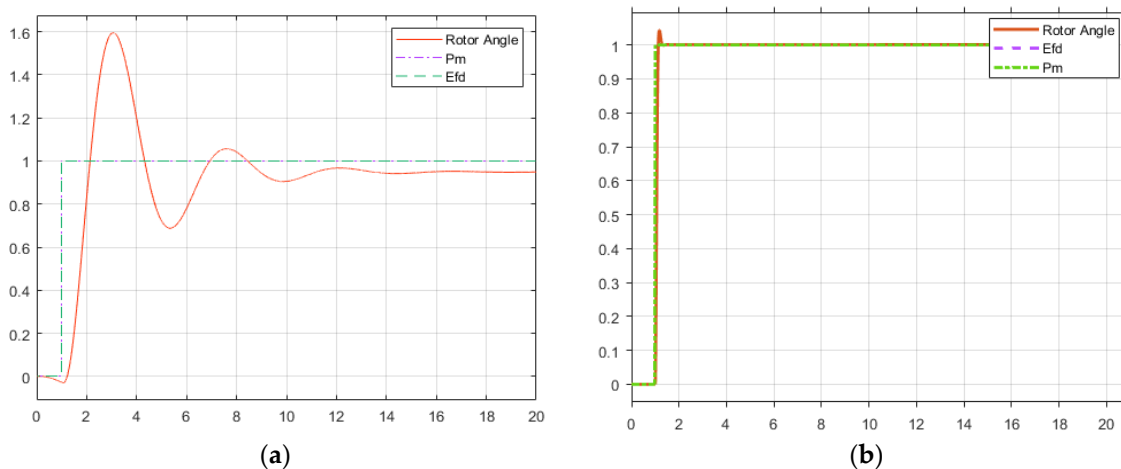


Figure 6. Rotor angle’s response when $E_{FD} = 1, P_m = 1$. (a) The Lyapunov-based trajectory tracking controller is applied to the system; (b) The MRAC is applied to the system.

Case study 1: Steady State

Case study 2: Fault at $t = 9$ s

Case study 3: Disturbances and Setpoint Change

A normally (Gaussian) distributed random signal with a variance of 1 and a 0.001 sample time was added onto the system. The noise was included at the start of the simulation to better replicate the inter-area oscillations that are inherent in a specific power system. A fault with the same characteristics as in Figure 7a was also applied to the system. Lastly, new setpoints were used with $E_{FD} = 2.395$, $P_m = 0.77778$.

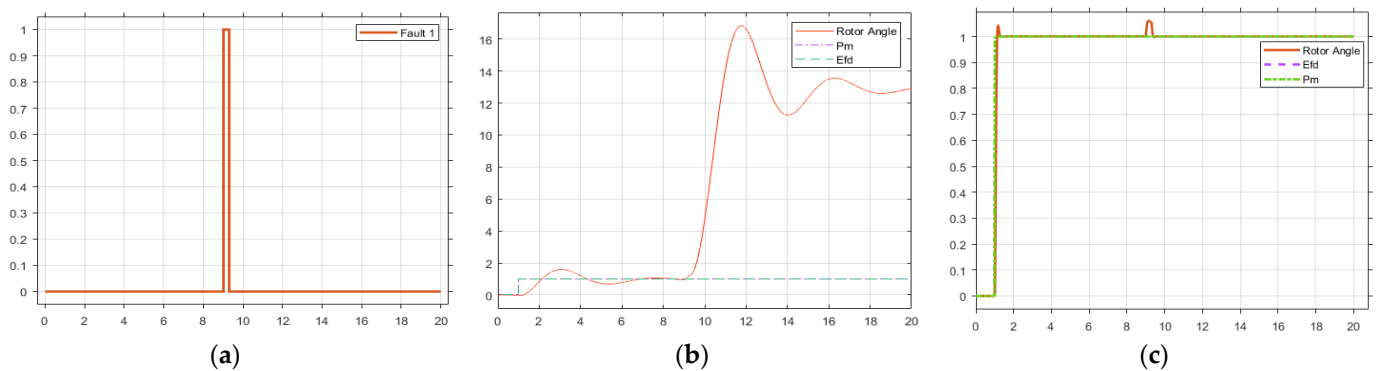


Figure 7. Rotor angle's response when $E_{FD} = 1$, $P_m = 1$, and a 300ms fault at $t = 9$ s. (a) Fault characteristics; (b) the Lyapunov-based trajectory tracking controller is applied to the system; (c) the MRAC is applied to the system.

The performances of both controllers are shown in Figure 8b,c.

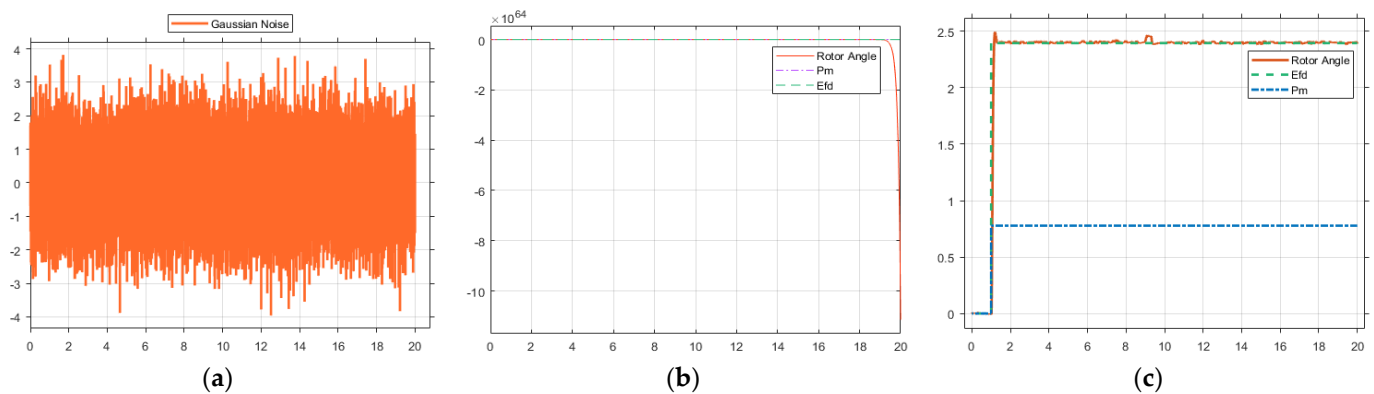


Figure 8. Rotor angle's response when $E_{FD} = 2.395$, $P_m = 1$, Gaussian noise, and a 300 ms fault at $t = 9$ s. (a) Gaussian noise characteristics; (b) the Lyapunov-based trajectory tracking controller is applied to the system; (c) the MRAC is applied to the system.

12. Discussion

To emulate the small variations in the loads that are mainly responsible for inter-area oscillations, disturbances in the form of Gaussian noise were added onto the system. To these disturbances, a 300 ms fault at $t = 9$ s as well as a setpoint change were also applied.

Using the Lyapunov-based trajectory tracking controller, most of the challenges stemmed from determining the appropriate gain to cause the system to behave in a similar way to the reference model. This is due to the limited amount of literature in that regard. Though it can be successfully used for wastewater control [19] and the nonlinear control of a Magnetic Levitation (Maglev) system [18], this controller did not yield good results for the synchronous generator rotor angle stability and control. As illustrated in Figure 7a, the rotor angle's response was somehow acceptable under the steady-state conditions, with it having a gain of 4.5. However, the changes in the setpoints as well as the introduction of

disturbances in the system showcased its limitations. Furthermore, the sensitivity of such a controller can easily be identified as the overall stability was lost when it was subjected to contingencies such as a fault (see Figure 7b) or small disturbances which emulated Gaussian noise (see Figure 8b).

In contrast to the Lyapunov-based controller, the MRAC maintained a significantly stable response with an overshoot of less than 5%, a rising time of less than 100 ms, no steady-state error, and a remarkable recovery time of less than 600 ms. With such results, this type of controller could be deployed efficiently as part of a decentralized control architecture with the aim of enhancing the (rotor) angle stability in a larger power system, thus, mitigating the effects of Low-Frequency Electromechanical Oscillations (LFEOs). Lastly, considering the time of interest from 3 s to 5 s for the standard power systems and 10 s for the larger ones with weak interconnections, the MRAC architecture is very robust. Table 1 summarises the various test cases with their corresponding results.

Table 1. Performance characteristics of the Lyapunov-based tracking controller and MRAC.

Case Studies	Controller	E_{FD}	P_m	Gaussian Noise	Fault	Rise Time (ms)	Overshoot (%)	Steady-State Error (%)	Recovery Time (ms)
Case 1	Lyapunov	1	1	No	No	649.504	66.949	0.0516	N/A
	MRAC	1	0	No	No	88.852	4.737	N/A	N/A
Case 2	Lyapunov	1	1	No	Yes	1044	35.507	11.88	N/A
	MRAC	1	1	No	Yes	84.207	4.147	N/A	~523
Case 3	Lyapunov	2.395	0.77778	Yes	Yes	N/A	N/A	N/A	N/A
	MRAC	2.395	0.77778	Yes	Yes	90.544	3.646	N/A	~550

13. Conclusions

This paper presented two control architectures for power system rotor angle stability enhancement, namely, a Lyapunov-based trajectory tracking one and an MRAC. Though it was fairly robust at the steady state, the first controller has been proven to be sensitive to contingencies such as faults. Moreover, the introduction of a normally (Gaussian) distributed random signal with a variance that was between 1 and 0.001 during the sample time, the rotor angle grew abruptly after the nineteenth second (19 s) to values that were in the range of $\geq 10^{64}$. In contrast with the Lyapunov-based architecture, the MRAC has been shown to be well suited to enhance the stability of the synchronous generator rotor angle when it was subjected to faults, setpoint changes, as well as disturbances in the form of noise that emulate variations in the load. The results which were obtained with the direct adaptive concept are consistent with those presented in [27].

14. Recommendations

Though it was shown to be less suitable for rotor angle stability when it was used alone without any PSS, the Lyapunov-based trajectory tracking controller can be explored on the 4th order model of the synchronous generator. The results that were obtained could either confirm its unsuitability for power system rotor angle control or limit it to a 4th order model representation, for instance. In light of the results in [29], this controller could also be used in conjunction with PSSs to further assess its performance. Given the lack of literature regarding the computation of a suitable gain, the real-time implementation of the Lyapunov-based controller may be challenging. As for the MRAC, its real-time implementation with a single SMIB configuration, then, in a multi-machine power system as part of a decentralized control architecture could confirm or not confirm the irrelevance of the PSSs when this adaptation algorithm is deployed. Moreover, the use of Flexible alternating Current Transmission System (FACTS) devices to enhance stability could also be examined and conclusions could be drawn.

Author Contributions: Conceptualization, T.-w.P.-P.B.-B., Y.D.M. and C.K.; methodology, T.-w.P.-P.B.-B.; software, T.-w.P.-P.B.-B.; validation, T.-w.P.-P.B.-B.; formal analysis, T.-w.P.-P.B.-B.; investigation,

T.-w.P.-P.B.-B.; resources, T.-w.P.-P.B.-B., Y.D.M. and C.K.; data curation, T.-w.P.-P.B.-B.; writing—original draft preparation, T.-w.P.-P.B.-B.; writing—review and editing, T.-w.P.-P.B.-B.; visualization, T.-w.P.-P.B.-B.; supervision, Y.D.M. and C.K. All authors have read and agreed to the published version of the manuscript.

Funding: This research received no external funding.

Data Availability Statement: Not applicable.

Conflicts of Interest: The authors declare no conflict of interest.

Appendix A. Generator Parameters

Table A1. Synchronous generator parameters [22].

Acronym/Parameter	Value
x_d	1.8 p.u
x'_d	0.3 p.u
x_q	1.7 p.u
x'_q	0.55 p.u
x''_q	0.25 p.u
x''_d	0.25 p.u
D	0
H	6.5
S	900 MVA
T'_{q0}	0.4 s
T''_{d0}	8 s
T''_{q0}	0.03 s
T'''_{q0}	0.05 s
Adaptation rate interval	[2, 100]
Optimal Lyapunov Gain	4.5

References

1. Nguyen, N.T. *Advanced Textbooks in Control and Signal Processing Model-Reference Adaptive Control A Primer*; Springer International Publishing: Berlin, Germany, 2018; ISBN 978-3-319-56393-0.
2. Slotine, J.-J.E.; Li, W. *Applied Nonlinear Control*; Prentice Hall: Hoboken, NJ, USA, 1991; ISBN 0-13-040890-5.
3. Grayson, L.P. The Status of Synthesis Using Lyapunov's Method. *Automatica* **1965**, *3*, 91–121. [[CrossRef](#)]
4. Bosworth, J.T.; Williams-Hayes, P.S. Flight Test Results from the NF-15B Intelligent Flight Control System (IFCS) Project with Adaptation to a Simulated Stabilator Failure. In Proceedings of the 2007 AIAA InfoTech at Aerospace Conference, Rohnert Park, CA, USA, 7–10 May 2007; Collection of Technical Papers. American Institute of Aeronautics and Astronautics: Reston, VA, USA, 2007; Volume 2, pp. 1080–1097. [[CrossRef](#)]
5. Williams-Hayes, P.S. Flight Test Implementation of a Second-Generation Intelligent Flight Control System. In Proceedings of the 2005 Infotech@ Aerospace Conference, Arlington, VA, USA, 26–29 September 2005.
6. Calise, A.J.; Rysdyk, R.T. Nonlinear Adaptive Flight Control Using Neural Networks. *IEEE Control Syst.* **1998**, *18*, 14–25. [[CrossRef](#)]
7. Narendra, K.S.; Annaswamy, A.M. Persistent Excitation in Adaptive Systems. *Int. J. Control* **1987**, *45*, 127–160. [[CrossRef](#)]
8. Rogers, G. *Power System Oscillations*; Springer Science and Business Media: New York, NY, USA, 2000.
9. Banga-Banga, T.P. Model Reference Adaptive Control Algorithm for Power System Interarea Oscillations Damping. Master's Thesis, Cape Peninsula University of Technology, Cape Town, South Africa, 2022.
10. Kamwa, I.; Trudel, G.; Gerin-Lajoie, L. Robust Design and Coordination of Multiple Damping Controllers Using Nonlinear Constrained Optimization. In Proceedings of the 21st IEEE International Conference on Power Industry Computer Applications. Connecting Utilities, Santa Clara, CA, USA, 21 May 1999; pp. 87–94. [[CrossRef](#)]
11. Hashmani, A.A.; Erlich, I. Mode Selective Damping of Power System Electromechanical Oscillations for Large Power Systems Using Supplementary Remote Signals. *Int. J. Electr. Power Energy Syst.* **2012**, *42*, 605–613. [[CrossRef](#)]
12. Banga-Banga, T.P.; Adewole, A.C.; Tzoneva, R. Oscillation Mode Estimation Using Spectrum Analysis of Synchronized Phasor Measurements. In Proceedings of the South African Universities Power Engineering Conference (SAUPEC), Cape Town, South Africa, 11 September 2017; pp. 818–823.
13. Wei, Q.; Han, X.; Guo, W.; Yang, M.; He, N. The Principle of Absolute Rotor Angle Control and Its Effect on Suppressing Inter-Area Low Frequency Oscillations. *Int. J. Electr. Power Energy Syst.* **2014**, *63*, 1039–1046. [[CrossRef](#)]

14. Wei, Q.; Guo, W.; Han, X.; Guo, M. Generator Rotor Angle Droop Control and Its Load-Following Characteristics. In Proceedings of the 2016 IEEE International Conference on Power System Technology (POWERCON 2016), Wollongong, Australia, 28 September–1 October 2016. [\[CrossRef\]](#)
15. Yohanandhan, R.V.; Srinivasan, L. Decentralized Measurement Based Adaptive Wide-Area Damping Controller for a Large-Scale Power System. In Proceedings of the 2018 IEEE International Conference on Power Electronics, Drives and Energy Systems (PEDES 2018), Chennai, India, 18–21 December 2018. [\[CrossRef\]](#)
16. Elsayed, M.; Hammad, A.; Hafez, A.; Mansour, H. Real Time Trajectory Tracking Controller Based on Lyapunov Function for Mobile Robot. *Int. J. Comput. Appl.* **2017**, *168*, 8887. [\[CrossRef\]](#)
17. Kubo, R.; Fujii, Y.; Nakamura, H. Control Lyapunov Function Design for Trajectory Tracking Problems of Wheeled Mobile Robot. *IFAC PapersOnLine* **2020**, *53*, 6177–6182. [\[CrossRef\]](#)
18. Mfoumboulou, Y.D.; Mnguni, M.E.S. Development of a New Linearizing Controller Using Lyapunov Stability Theory and Model Reference Control. *Indones. J. Electr. Eng. Comput. Sci.* **2022**, *25*, 1328–1343. [\[CrossRef\]](#)
19. Nketoane, P.A. Design and Implementation of a Nonlinear Controller in PLC as Part of an Adroid Scada System for Optimal Adaptive Control of the Activated Sludge Process. Master's Thesis, Cape Peninsula University of Technology, Cape Town, South Africa, 2009.
20. Ghosh, A.; Ledwich, G.; Malik, O.P.; Hope, G.S. Power System Stabilizer Based on Adaptive Control Techniques. *IEEE Trans. Power Appar. Syst.* **1984**, *8*, 1983–1989. [\[CrossRef\]](#)
21. Fan, J.Y.; Ortmeyer, T.H.; Mukundan, R. Power System Stability Improvement with Multivariable Self-Tuning Control. *IEEE Trans. Power Syst.* **1990**, *5*, 227–234. [\[CrossRef\]](#)
22. Eremia, M.; Shahidehpour, M. *Handbook of Electrical Power System Dynamics: Modeling, Stability, and Control*; John Wiley and Sons: Hoboken, NJ, USA, 2013.
23. Kim, K.H. Model Reference Adaptive Control-Based Adaptive Current Control Scheme of a PM Synchronous Motor with an Improved Servo Performance. *IET Electr. Power Appl.* **2009**, *3*, 8–18. [\[CrossRef\]](#)
24. Mosaad, M.I. Model Reference Adaptive Control of STATCOM for Grid Integration of Wind Energy Systems. *IET Electr. Power Appl.* **2018**, *12*, 605–613. [\[CrossRef\]](#)
25. Wu, H.; Wang, X. A Mode-Adaptive Power-Angle Control Method for Transient Stability Enhancement of Virtual Synchronous Generators. *IEEE J. Emerg. Sel. Top. Power Electron.* **2020**, *8*, 1034–1049. [\[CrossRef\]](#)
26. Bhunia, M.; Subudhi, B.; Ray, P.K. Design and Real-Time Implementation of Cascaded Model Reference Adaptive Controllers for a Three-Phase Grid-Connected PV System. *IEEE J. Photovolt.* **2021**, *11*, 1319–1331. [\[CrossRef\]](#)
27. Abubakr, H.; Vasquez, J.C.; Hassan Mohamed, T.; Guerrero, J.M. The Concept of Direct Adaptive Control for Improving Voltage and Frequency Regulation Loops in Several Power System Applications. *Int. J. Electr. Power Energy Syst.* **2022**, *140*, 108068. [\[CrossRef\]](#)
28. Abd El-Kareem, A.H.; Abd Elhameed, M.; Elkholy, M.M. Effective Damping of Local Low Frequency Oscillations in Power Systems Integrated with Bulk PV Generation. *Prot. Control. Mod. Power Syst.* **2021**, *6*, 41. [\[CrossRef\]](#)
29. Robak, S.; Bialek, J.W.; Machowski, J. Comparison of Different Control Structures for Lyapunov-Based Power System Stabilizer. In Proceedings of the IEEE Power Industry Computer Applications Conference, Sydney, Australia, 20–24 May 2001; pp. 229–234.
30. Khalil, H.K. *Nonlinear Systems*; Pearson Education: London, UK, 2001; ISBN 978-0-13-067389-3.
31. Sastry, S.; Bodson, M. *Adaptive Control—Stability, Convergence, and Robustness*; Thomas Kailath, Ed.; Prentice Hall: New Jersey, NJ, USA, 1989.
32. Machowski, J.; Lubosny, Z.; Bialek, J.W.; Bumby, J.R. *Power System Dynamics: Stability and Control*; Wiley and Sons: Hoboken, NJ, USA, 2008; ISBN 978-1-119-96505-3.
33. Kundur, P. *Power System Stability and Control*; McGraw-Hill Education: New York, NY, USA, 1994; p. 1176.
34. Scott, B. Power System Dynamics Response Calculations. *Proceeding IEEE* **1979**, *67*, 219–241.
35. De León-Morales, J.; Busawon, K.; Acosta-Villarreal, G.; Acha-Daza, S. Nonlinear Control for Small Synchronous Generator. *Int. J. Electr. Power Energy Syst.* **2001**, *23*, 1–11. [\[CrossRef\]](#)
36. Sanchez-Orta, A.E.; De León-Morales, J.; Lopez-Toledo, E. Discrete-Time Nonlinear Control Scheme for Small Synchronous Generator. *Int. J. Electr. Power Energy Syst.* **2002**, *24*, 751–764. [\[CrossRef\]](#)
37. Zacharia, L.; Asprou, M.; Kyriakides, E. Wide Area Control of Governors and Power System Stabilizers with an Adaptive Tuning of Coordination Signals. *IEEE Open Access J. Power Energy* **2020**, *7*, 70–81. [\[CrossRef\]](#)
38. Ghahremani, E.; Kamwa, I. Local and Wide-Area PMU-Based Decentralized Dynamic State Estimation in Multi-Machine Power Systems. *IEEE Trans. Power Syst.* **2016**, *31*, 547–562. [\[CrossRef\]](#)
39. Su, S.J.; Zhu, Y.Y.; Wang, H.R.; Yun, C. A Method to Construct a Reference Model for Model Reference Adaptive Control. *Adv. Mech. Eng.* **2019**, *11*, 1687814019890455. [\[CrossRef\]](#)